

# Quantum theory of phase correlations in optical frequency combs generated by stimulated Raman scattering

Chunbai Wu,<sup>1</sup> M. G. Raymer,<sup>1</sup> Y. Y. Wang,<sup>2</sup> and F. Benabid<sup>2</sup>

<sup>1</sup>*Department of Physics, Oregon Center for Optics, University of Oregon, Eugene, Oregon 97403, USA*

<sup>2</sup>*Gas-Phase Photonic Materials Group, Centre for Photonics and Photonic Materials, University of Bath,*

*Claverton Down, Bath, BA2 7AY, United Kingdom*

(Received 30 July 2010; published 29 November 2010)

We explore theoretically the phase correlation between multiple generated sidebands in a Raman optical frequency comb under conditions of spontaneous initiation from quantum zero-point noise. We show that there is a near-deterministic correlation between sideband phases in each laser shot which may lead to synthesis of attosecond pulse trains.

DOI: [10.1103/PhysRevA.82.053834](https://doi.org/10.1103/PhysRevA.82.053834)

PACS number(s): 42.65.Dr, 42.50.Ct, 42.62.Eh

## I. INTRODUCTION

Stimulated Raman scattering (SRS) has been widely used to produce optical frequency comb spectra in recent research efforts that aim to synthesize femtosecond or attosecond optical pulses. This requires phase-locked (mutually coherent) comb lines that span a spectral range of the order of 1000 THz or larger (e.g., from near UV to near ir). The first experiment toward this goal was done using hydrogen gas in which multiple stimulated rotational Raman orders were observed and analyzed under pumping by high-power femtosecond pulses [1]. Shortly afterward, a two-Raman-pump scheme was proposed where the medium's Raman coherence is driven slightly off resonance and results in a Raman comb spectrum with Bessel-function amplitudes and phases [2]. Experiments following this scheme successfully produced single-cycle optical pulses by adjusting the relative phase between each comb component [3]. Further efforts in controlling the carrier envelope phase (CEP) of the generated single-cycle pulses [4] as well as to generate constant CEP pulse trains [5,6] were later realized.

In parallel developments, hollow-core photonic crystal fiber (HC-PCF) with kagome lattice was developed, showing an ultrabroad transmission bandwidth spanning multiple octaves [7]. This fiber is useful in generating Raman combs for several reasons: A Raman-active medium like hydrogen gas at high pressure can be sealed inside the core of the fiber and made to interact strongly with the guided pump laser beam, tightly confined to an effective core area of about  $10\ \mu\text{m}$ . This ensures the pump intensity as well as the Raman interaction region are strongly enhanced compared with the conventional free-space Raman experiments using spherical lenses to focus the pump. As a result of this, the strongly transient regime of Raman generation was demonstrated with a pump pulse duration much larger than the dephasing time of the Raman transition [8]. In addition, the dispersion of the guided modes is low enough so that nearly phase-matched four-wave mixing can take place between the many spectral lines comprising the frequency comb.

More than 40 Raman rotational and vibrational lines in hydrogen gas have been observed [9] by coupling 12-ns-duration pump pulses into kagome HC-PCF. The mechanism creating the comb is as follows: SRS induced by the pump builds up from spontaneous Raman scattering, producing the first pair of Stokes and anti-Stokes-shifted fields. When these fields grow to sufficient intensities, they act as new pumps, creating the next higher order of sidebands. This process

ascades, producing many sideband pairs with frequencies shifted from the pump frequency by multiples of the fundamental molecular-vibration resonance frequency  $\omega_R$ . The cascaded Raman process is highly nonlinear, as initially weak, spontaneously emitted fields grow to become comparable in strength to the input pump field. Due to the inherent spontaneous initiation of Raman scattering, the Stokes field is known to undergo quantum fluctuations from one pump pulse to another [10]. These fluctuations occur not only in the energy of the Stokes field, but also its temporal phase [11].

These advances in experiments show the promising future of using Raman combs to synthesize ultrashort optical pulses. But a fundamental issue that has not been explored theoretically in Raman comb generation is the nature of the spontaneously occurring phase correlations between the Raman comb components. Are the comb line phases statistically independent? If they are correlated, do these correlations tend to enhance or to hinder the formation of ultrashort pulses through the interference of all the lines? Experiments using long pump pulses (200 ps to 12 ns) provide strong evidence of such an automatic phase locking that tends to enhance formation of ultrashort pulses [12,13]. Earlier experiments using subpicosecond pump pulses also indicated phase correlation creating ultrashort pulses, but in that case it is not clear if the molecular coherence was initiated spontaneously or was seeded through impulsive Raman scattering [14].

In this paper we develop the quantum theory of multiline Raman combs initiated from spontaneous Raman scattering and amplified by SRS. The theory confirms this spontaneously generated phase correlation between the Raman comb components in the transient high-gain regime, assuming a single pump pulse with no pump depletion. Through theoretical analysis, incorporating quantum fluctuations in a careful manner, we find simple relationships predicting the nature of these correlations. We predict that under ideal conditions, all the comb lines correspond to transform-limited pulses that automatically become nearly perfectly phase locked among themselves, leading to the possibility of generating attosecond pulses. This “self”-phase locking occurs in the absence of a second pump field or any other mechanism for classical injection of coherence. In particular, using a rigorous solution of the quantum Maxwell-Bloch equations for the problem, we predict that the first-order Stokes and anti-Stokes lines are very strongly phase anticorrelated throughout the duration of these

two pulses, even in the situation where large phase-velocity dispersion is present in the medium. We associate this phase anticorrelation with the requirement for producing maximum Raman vibrational (or rotational) coherence in the medium, which acts as a phase-sensitive amplifier. For the higher-order Raman components, we use two simplified models to predict their phase relations, both of which are consistent with a simple quantitative formula for the phase relations:  $\theta_n = \theta_p + n\phi + \delta_n$ , where  $\theta_p$  is the phase of the pump pulse,  $\phi$  is a single random phase characteristic of the amplified spontaneous initiation process,  $n$  is the order of the Stokes line, and  $\delta_n$  is a deterministic phase shift specific to each line. Such phase relations naturally lead to formation of ultrashort pulses if all deterministic phase shifts are adjusted to appropriate values, as in [3].

The result also reveals that if the frequency of each comb component is controlled to be an exact integer multiple of the Raman-shift frequency, then a periodic pulse train [6] with constant CEP will be synthesized by the Raman comb created from each separate pump pulse. However, because of the inherent spontaneous initiation of Raman scattering, the CEP of the synthesized pulse train will vary with each pump pulse, preventing stable formation of single-cycle pulses in the train. We propose to simultaneously use the pump and its second harmonic, which happens to be one of the anti-Stokes fields in the Raman comb, to interact with the medium so that the synthesized pulse trains are locked to one deterministic CEP. Dual pumping of this type has been explored experimentally [5,6], but with the added complexity of externally injecting Raman coherence into the system with additional coherent laser fields.

## II. QUANTUM THEORY OF CASCADED RAMAN SCATTERING IN HIGH-GAIN REGIME

Previous theoretical and experimental work on Raman scattering has shown that if the scattering takes place in the strongly transient, high-gain regime (where the pump pulse is much shorter than the effective vibrational dephasing time) and its Fresnel number is close to unity, then the Stokes field generated by a single pump pulse is temporally and spatially coherent within a single shot of the laser [9,10]. We refer to this as ‘‘shot coherence.’’ Shot-to-shot fluctuations of field phase and energy

occur, and are well explained by theory [10,11,15–17]. This suggests that the generated first-Stokes field is a transform-limited pulse with a well-defined temporal phase. We extend these considerations to a wide-band Raman optical comb.

We consider the following experimental setup that is discussed in [9] as our theoretical model: A single long pump pulse is coupled into the microstructured hollow-core fiber, and stimulates the generation of Raman sidebands as it interacts with hydrogen molecules that have been filled in the fiber core. By ‘‘long’’ we mean that the pulse has a narrow bandwidth (much less than the Raman-shift frequency) so it does not impulsively excite any molecular coherence. The cascading Raman comb generation process is illustrated in Fig. 1, and the frequency of each comb component obeys the following relation as required by energy conservation:

$$\omega_n = \omega_0 + n\omega_R, \quad (1)$$

where  $\omega_0$  is the pump frequency,  $n$  denotes the  $n$ th sideband ( $n > 0$  for anti-Stokes,  $n = 0$  for pump, and  $n < 0$  for Stokes), and  $\omega_R$  is the Raman-shift frequency (either pure vibrational or pure rotational). In our analysis we assume that molecules are evenly distributed within the fiber core and that the fiber confines all relevant Raman frequencies in single transverse modes in its core area  $A$ , as it has been shown in kagome fiber [9]. This allows us to safely assume that a one-dimensional theory is sufficient to analyze the properties of generated Stokes and anti-Stokes fields [16].

The interaction Hamiltonian for the system, including all electric fields and the molecular vibrational modes can be written as (see Appendix A)

$$H_I = -AN \sum_n \int dz \{ \alpha_{1,n} P(z,t) E_n^{(+)}(z,t) E_{n-1}^{(-)}(z,t) e^{i\Delta\beta_n z} + \alpha_{1,n+1}^* P^\dagger(z,t) E_n^{(+)}(z,t) E_{n+1}^{(-)}(z,t) e^{-i\Delta\beta_{n+1} z} \}, \quad (2)$$

where  $E_n$  is the quantized field operator for the slowly varying envelope of the  $n$ th sideband,  $P(z,t)$  is the raising operator for collective molecular vibration at position  $z$ , and  $\alpha_{1,n}$  is the complex coupling efficiency that is related to the Kramers-Heisenberg cross-section coefficient for the producing  $n$ th sideband. We also have included the differences between the

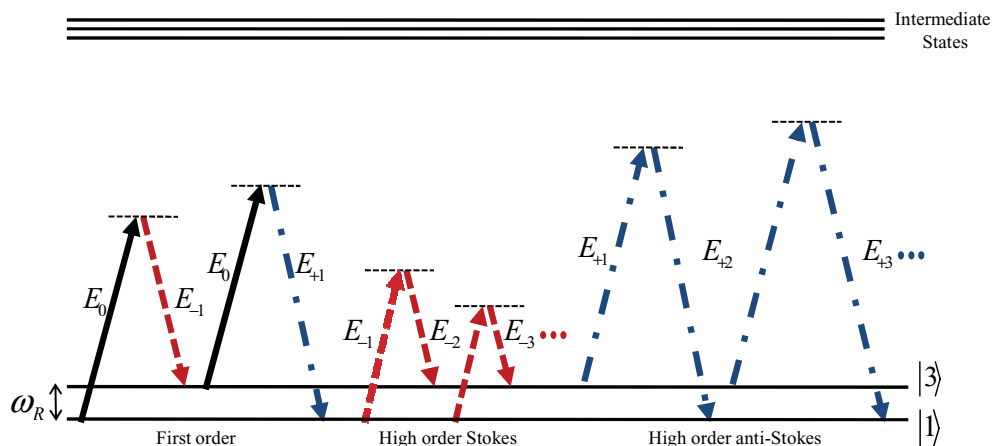


FIG. 1. (Color online) Raman comb generation process. Stokes (anti-Stokes) fields are indicated by dashed (dot-dash) arrows. The ground (first-excited) molecular eigenstates are indicated by  $|1\rangle(|3\rangle)$ .

propagation constants of adjacent Raman lines through the fiber, denoted as  $\Delta\beta_n = \beta_n - \beta_{n-1}$ . We neglect the molecular rotational excitation, which would be included by a separate, independent variable analogous to  $P(z, t)$ . We also assume each frequency mode is characterized by a single optical polarization state (linear for vibrational scattering).

The quantized slowly varying electric field operators are related to the photon creation and annihilation operators  $a_n(z, t)$  by (in Gaussian units):

$$E_n^{(-)}(z, t) = i\sqrt{\frac{2\pi\hbar\omega_n}{AL}}a_n^\dagger(z, t), \quad (3)$$

where  $L$  is the fiber length. The collective molecular-vibration raising operator at location  $z$  is defined as

$$P(z, t) = 1/(NA) \sum_{\{m\}} \sigma_{31}^m(t), \quad (4)$$

where  $\sigma_{31}^m(t)$  is the raising operator for the  $m$ th molecule located within a volume cell at position  $z$ , which excites the molecule from ground state  $|1\rangle$  to vibrational state  $|3\rangle$ .  $N$  is the molecular number density. For review of the quantum SRS theory, see [15].

The Maxwell-Bloch equations of motion for the electric-field operators  $E_n$  of each individual comb line and the collective molecular vibration raising operator  $P$  can be derived by using Eq. (2) (see Appendix A):

$$\begin{aligned} \partial_z E_n^{(-)}(z, \tau) &= -i\alpha_{2,n+1} E_{n+1}^{(-)} \exp(-i\Delta\beta_{n+1}z) P^\dagger \\ &\quad - i\alpha_{2,n}^* E_{n-1}^{(-)} \exp(i\Delta\beta_n z) P, \quad (5) \\ \partial_\tau P^\dagger(z, t) &= i \sum_{n=-N}^N \alpha_{1,n} E_n^{(+)} E_{n-1}^{(-)} \exp(i\Delta\beta_n z) - \Gamma P^\dagger + F_\Gamma, \end{aligned}$$

where  $\alpha_{2,n} = 2\pi\hbar N\omega_n\alpha_{1,n}^*/c$ , while  $F_\Gamma$  and  $\Gamma$  are the quantum Langevin operator and damping rate associated with dephasing collisions, and  $\tau = t - z/c$  is the local time variable. Equation (5) is consistent with earlier formulations in which phase mismatch or multilines were omitted [18,19].

Equation (5) is nonlinear while involving all the Raman sidebands. As a simplifying case, we first consider the situation where only first-order Stokes  $E_{-1}$  and anti-Stokes  $E_{+1}$  fields are created, and the pump intensity profile is unchanged throughout the interaction. This simplified linear model allows us to find a complete quantum description and gain insight into the comb generation process. In the high-gain, transient regime we can neglect the Langevin operator and damping [15]. Then the coupled equations are

$$\begin{aligned} \partial_z E_{-1}^{(-)}(z, \tau) &= -i\alpha_{2,s} E_0(\tau) P^\dagger(z, \tau), \\ \partial_z E_{+1}^{(+)}(z, \tau) &= i\alpha_{2,a} E_0^*(\tau) P^\dagger(z, \tau) \exp(-i\Delta\beta z), \quad (6) \\ \partial_\tau P^\dagger(z, \tau) &= i\alpha_{1,s} E_{-1}^{(-)}(z, \tau) E_0^*(\tau) \\ &\quad + i\alpha_{1,a} E_{+1}^{(+)}(z, \tau) E_0(\tau) \exp(i\Delta\beta z), \end{aligned}$$

where  $\Delta\beta = \beta_1 + \beta_{-1} - 2\beta_0$  is the phase mismatch of wave vectors. These coupled equations were first solved in a full quantum context by Kilin [20], who verified that a slight phase mismatch is needed to maximize the generation of Stokes or anti-Stokes sideband generation, as seen in experiments [21]. More general solutions than those in [20] are found here using the methods in [19]. Assuming that the pulses are long enough that group-velocity effects are not important, the field operators at the end of the fiber ( $z = L$ ) and at local time  $\tau = t - z/v_g$  (where  $v_g$  is the group velocity of the pump) are found to be

$$\begin{aligned} \begin{bmatrix} E_{-1}^{(-)}(L, \tau) \\ E_{+1}^{(+)}(L, \tau) \end{bmatrix} &= E_0(\tau) \int_0^\tau d\tau' E_0(\tau') \begin{bmatrix} \alpha_{2,s} G_{11}(L; \tau, \tau') & \alpha_{2,s} G_{12}(L; \tau, \tau') \\ -\alpha_{2,a} G_{21}(L; \tau, \tau') & -\alpha_{2,a} G_{22}(L; \tau, \tau') \end{bmatrix} \begin{bmatrix} \alpha_{1,s} E_{-1}^{(-)}(0, \tau') \\ \alpha_{1,a} E_{+1}^{(+)}(0, \tau') \end{bmatrix} \\ &\quad + E_0(\tau) \int_0^L dz' \begin{bmatrix} -i\alpha_{2,s} G_{13}(z'; \tau, 0) \\ i\alpha_{2,a} G_{23}(z'; \tau, 0) \end{bmatrix} P^\dagger(L - z', 0) + \begin{bmatrix} E_{-1}^{(-)}(0, \tau) \\ E_{+1}^{(+)}(0, \tau) e^{i\Delta\beta L} \end{bmatrix}, \\ P^\dagger(L, \tau) &= i \int_0^\tau d\tau' \{ \alpha_{1,s} E_0^*(\tau') G_{13}(L; \tau, \tau') E_{-1}^{(-)}(0, \tau') + \alpha_{1,a} E_0(\tau') G_{13}(L; \tau, \tau') E_{+1}^{(+)}(0, \tau') \} \\ &\quad + \int_0^L dz' G_0(z'; \tau, 0) P^\dagger(L - z', 0). \quad (7) \end{aligned}$$

The Green propagators are given by

$$\begin{aligned} G_{11}(z; \tau, \tau') &= G_{12}(z; \tau, \tau') - i\Delta\beta \int_0^z dz' G_{12}(z'; \tau, \tau'); \\ G_{22}(z; \tau, \tau') &= G_{12}(z; \tau, \tau') + i\Delta\beta \exp(i\Delta\beta z) * G_{12}(z; \tau, \tau'); \\ G_{12}(z; \tau, \tau') &= G_{21}(z; \tau, \tau') = I_0(2\sqrt{\xi_s(\tau, \tau')z}) * [J_0(2\sqrt{\xi_a(\tau, \tau')z}) \exp(i\Delta\beta z)]; \\ G_{13}(z; \tau, \tau') &= I_0(2\sqrt{\xi_s(\tau, \tau')z}) * [\delta(z) - J_1(2\sqrt{\xi_a(\tau, \tau')z}) \sqrt{\xi_a(\tau, \tau')/z} \exp(i\Delta\beta z)]; \\ G_{23}(z; \tau, \tau') &= [I_1(2\sqrt{\xi_s(\tau, \tau')z}) \sqrt{\xi_s(\tau, \tau')/z} + \delta(z)] * [J_0(2\sqrt{\xi_a(\tau, \tau')z}) \exp(i\Delta\beta z)]; \\ G_0(z; \tau, \tau') &= [I_1(2\sqrt{\xi_s(\tau, \tau')z}) \sqrt{\xi_s(\tau, \tau')/z} + \delta(z)] * [\delta(z) - J_1(2\sqrt{\xi_a(\tau, \tau')z}) \sqrt{\xi_a(\tau, \tau')/z} \exp(i\Delta\beta z)], \end{aligned}$$

where “ $\ast$ ” denotes convolution on the variable  $z$ , and  $J_n, I_n$  are  $n$ th-order Bessel and modified Bessel functions, respectively. The time-dependent gain coefficients are

$$\xi_{s,a}(\tau, \tau') = \alpha_{1,(s,a)} \alpha_{2,(s,a)} \int_{\tau'}^{\tau} dt |E_0(t)|^2. \quad (8)$$

With the sideband fields initially in the vacuum state and all molecules in their lowest-energy states  $|1\rangle$ , the initial operators have the following correlation functions [19]:

$$\begin{aligned} \langle P^\dagger(z, 0) P(z', 0) \rangle &= (1/AN) \delta(z - z'), \\ \langle P(z, 0) P^\dagger(z', 0) \rangle &= 0, \\ \langle E_n^{(+)}(0, \tau') E_n^{(-)}(0, \tau) \rangle &= (2\pi \hbar \omega_n / Ac) \cdot \delta(\tau - \tau'), \\ \langle E_n^{(-)}(0, \tau') E_n^{(+)}(0, \tau) \rangle &= 0, n = \pm 1. \end{aligned} \quad (9)$$

Equation (7) represents two types of processes: The terms coupling  $E_{-1}^{(-)}$  ( $E_{+1}^{+}$ ) with  $P$  represent Stokes (anti-Stokes) scattering from ground-state (excited-state) molecules. The off-diagonal terms in the green matrix coupling  $E_{-1}^{(-)}$  with  $E_{+1}^{+}$  represent Stokes or anti-Stokes four-wave mixing, in which two pump photons are annihilated and an S/AS photon pair are created. Both of these processes drive the same collective molecular excitation  $P$ . The phases of the initiating vacuum (zero-point) fields are temporally and spatially fluctuating, as shown in the delta correlation functions of Eq. (9), which represents white noise in time and space. We could attribute this fluctuation to a thermal-like field distribution of the temporal-spatial modes (TSM) of the spontaneously emitted Stokes field, or equivalently to the thermal-like distribution of longitudinal spatial modes of the collective molecular excitation [17,23]. The laser field further scatters from the collective molecular excitation creating additional anti-Stokes light. Subsequently, the initial white noise is heavily filtered under the high-gain transient conditions, since the gain process is a resonant one, and the Green propagators grow exponentially as the pulse propagates through the medium. The filtering or smoothing process eventually produces a Stokes and anti-Stokes field that are determined solely by a single TSM each; in other words, each has the form of a smooth, transform-limited wave packet with an overall phase and a peak amplitude that are random from one pump pulse to another. In this sense, these two fields resemble classical fields, that is, complex temporal envelopes with well-defined carrier frequencies, although the intensities and phases of both fields dramatically fluctuate from one shot to another [10,11,23]. It is further known that if the scattering process goes into saturation, then the magnitude of the intensity fluctuations greatly decreases [22], although this is not accounted for in the linear theory considered here.

### III. ANTICORRELATION BETWEEN FIRST-ORDER STOKES AND ANTI-STOKES

Here we examine the mutual coherence between generated first-order Stokes (S1) and anti-Stokes (AS1) fields, in the high-gain transient regime. We calculate the correlation coefficient defined as

$$C = \frac{|\langle E_{-1}^{(-)}(L, \tau) E_{+1}^{(-)}(L, \tau) \rangle|^2}{\langle E_{-1}^{(-)}(L, \tau) E_{-1}^{(+)}(L, \tau) \rangle \langle E_{+1}^{(-)}(L, \tau) E_{+1}^{(+)}(L, \tau) \rangle}. \quad (10)$$

Because both fields in the numerator are negative-frequency ones, this gives the degree of phase anticorrelation between generated Stokes and anti-Stokes fields. Writing  $I_{\pm 1} = \langle E_{\pm 1}^{(-)} E_{\pm 1}^{(+)} \rangle$ , the phase correlation coefficient is proportional to the degree of mutual phase coherence, defined as  $C_\varphi = |\langle e^{-i(\varphi_{-1} + \varphi_{+1})} \rangle|$ , as is seen from

$$C = \frac{|\langle E_{-1}^{(-)} E_{+1}^{(-)} \rangle|^2}{I_{-1} I_{+1}} |\langle e^{-i(\varphi_{-1} + \varphi_{+1})} \rangle|^2,$$

if we assume that the fluctuations in intensities  $|E_{\pm 1}^{(-)}|^2$  of S1 and AS1 are independent of that of their phases. For example, if the temporal phase of the Stokes pulse is statistically independent of the anti-Stokes pulse, the  $C$  value (and  $C_\varphi$ ) would be zero. In contrast, if the sum of the phases of these two pulses stays constant from shot to shot (while they both fluctuate), which indicates phase anticorrelation, then  $C_\varphi$  would equal one, and  $C$  would be determined by intensity fluctuations alone.

By putting expressions from (7) into Eq. (10) and using the initial conditions (9), we calculate the  $C$  values under various conditions. The full expression is given in Appendix B. In Fig. 2 we plot  $C$  values and Stokes and anti-Stokes intensities as functions of local time  $\tau$  under the phase mismatch condition  $\Delta\beta L = 10$ , where the anti-Stokes intensity is maximized (see Fig. 3). In all our calculations here we use 12 ns [full width half maximum (FWHM)] transform-limited Gaussian pump pulses, and the Stokes and anti-Stokes integrated gain coefficients ( $\alpha_{1,s} \alpha_{2,s} \int_{-\infty}^{\infty} dt |E_0(t)|^2 L$ ) are set at the values of 25 and 30, respectively.

We see in Fig. 2 that the value of  $C$  nearly equals 1 throughout the duration of the generated Stokes pulses. Also note that the peak of the Stokes field is delayed by 4 ns relative to the peak of the pump field, which is consistent with previously known results [15]. In Fig. 3 we show the calculated  $C$  value at the peak of the Stokes-pulse intensity under various dispersion conditions, and find that its value stays close to 1. There we also show the peak Stokes and anti-Stokes-pulse

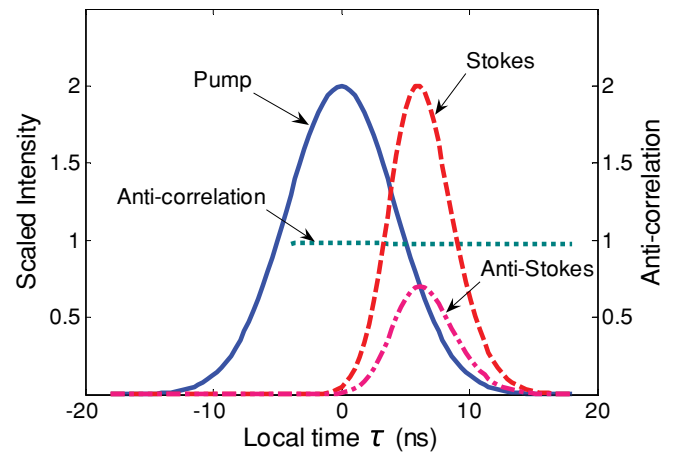


FIG. 2. (Color online) Pump and first-order Stokes and anti-Stokes mean intensities (scaled differently; Stokes scaled 5 times more than anti-Stokes), and their anticorrelation  $C$  as functions of local time.

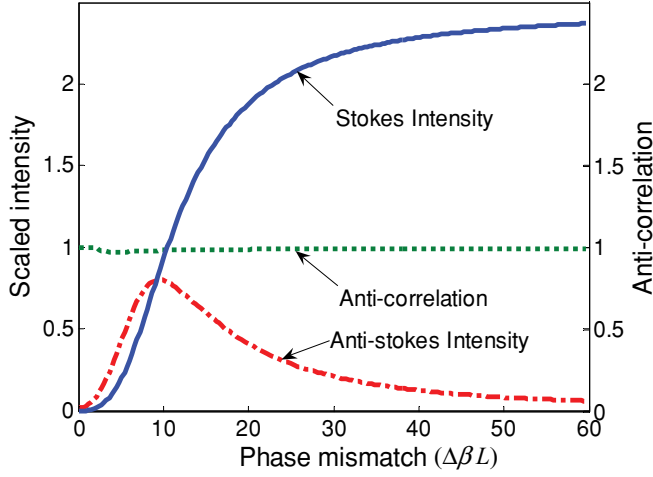


FIG. 3. (Color online) First-order Stokes and anti-Stokes mean intensities (scaled differently; Stokes scaled 10 times more than anti-Stokes), and their anticorrelation  $C$  as functions of phase mismatch.

intensities versus phase mismatch, showing the well-known minimum that occurs for perfect phase matching [20,21,24].

The result  $C \approx 1$  implies that the first-order Stokes and anti-Stokes are correlated in the following way:

$$E_{+1}^{(+)} \approx \alpha E_{-1}^{(-)},$$

where  $\alpha$  is a complex constant (with magnitude less than unity). This relation shows that, not only the intensities of the two sidebands fluctuate in the same manner from pulse to pulse, but their phases are near perfectly anticorrelated. This confirms one of our conjectures in [9]. It indicates a tendency in this system to automatically evolve toward perfect phase anticorrelation, although our experimental observations [12,13] show that the anticorrelation is not perfect. A more rigorous model including all comb lines and pump depletion is needed for explaining this discrepancy.

The generated sideband fields are also correlated with the collective molecular excitation created in the medium, as seen in the solution (7). The quantity  $\langle P(L, \tau) E_{-1}^{(-)}(L, \tau) \rangle$ , which is a measure of this field-medium correlation, is plotted in Fig. 4 as a function of the local time  $\tau$ . It shows a maximum in time, following the Stokes fields (see Fig. 2). This correlation between field and molecular coherence has been studied in experiment for the case that Stokes only was generated [17]. In the absence of dephasing processes, this nonzero correlation can be considered as a manifestation of quantum state entanglement between the medium and the fields.

#### IV. MECHANISM FOR PHASE LOCKING

Here we provide a simple, intuitive model that helps explain the physical mechanism of the automatic phase anticorrelation between first-order Stokes and anti-Stokes fields predicted above. It also predicts the phase relations among all comb lines, a result that is further supported by the independent calculation in the following section. Equation (5) can be simplified by assuming perfect phase matching, since the phase mismatch does not strongly affect the phase anticorrelation,

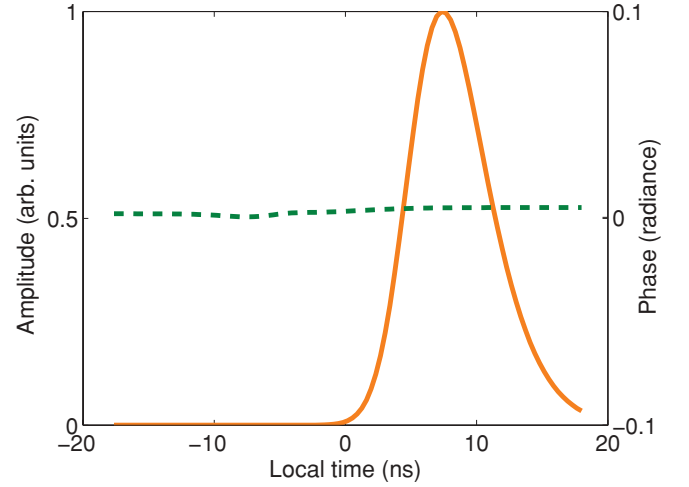


FIG. 4. (Color online) Amplitude and phase of quantity  $\langle P(L, \tau) E_{-1}^{(-)}(L, \tau) \rangle$ . Phase value is with respect to the pumps.

as shown in Fig. 3. We treat the fields as classical random processes, and define real amplitudes and phases by

$$E_n^{(-)} = |E_n^{(-)}| e^{-i\theta_n}, P = |P| e^{-i\phi'}. \quad (11)$$

This gives the evolution of the molecular polarization as

$$i|P|\partial_\tau\phi' + \partial_\tau|P| = \sum_{n=-N}^N |\alpha_{1,n}| |E_n^{(+)}| |E_{n-1}^{(-)}| e^{i(\theta_n - \theta_{n-1} - \phi' - \delta)}, \quad (12)$$

where we expressed the complex coefficient  $i\alpha_{1,n}$  in terms of an amplitude and phase:  $i\alpha_{1,n} = |\alpha_{1,n}| \exp(-i\delta)$ . This gives two real equations:

$$\begin{aligned} \partial_\tau|P| &= \sum_{n=-N}^N |\alpha_{1,n}| |E_n^{(+)}| |E_{n-1}^{(-)}| \cos(\theta_n - \theta_{n-1} - \phi' - \delta), \\ \partial_\tau\phi' &= \frac{1}{|P|} \sum_{n=-N}^N |\alpha_{1,n}| |E_n^{(+)}| |E_{n-1}^{(-)}| \sin(\theta_n - \theta_{n-1} - \phi' - \delta). \end{aligned} \quad (13)$$

The first equation in (13) implies that the molecular polarization grows at a maximal positive rate if  $\theta_n - \theta_{n-1} - \phi' - \delta = 0$ . In this situation, the second equation implies that the random phase  $\phi'$  of the molecular polarization becomes time independent, as the sin function goes to zero. This result is consistent with the established phenomenon of high-gain temporal filtering [17]. The idea is that the spontaneously generated comb lines can arise with any phase values, and the values that actually occur will be those leading to the highest overall gain, as indicated by the highest growth rate of  $|P|$ . This highest gain also leads to time-independent phases with particular relations among them. This is similar to self-mode locking in a laser. For compactness, this relation can be written as

$$\theta_n - \theta_{n-1} = \phi, \quad (14)$$

where  $\phi = \phi' + \delta$  absorbs the constant  $\delta$  into the random phase  $\phi'$ . The random variable  $\phi$  has uniform probability between 0 and  $2\pi$  [11]. For the case of a strong pump in

the  $n = 0$  mode with phase  $\theta_0$ , this relation implies for the anti-Stokes and Stokes phases,  $\theta_1 = \theta_0 + \phi$  and  $\theta_{-1} = \theta_0 - \phi$ . These further imply perfect anticorrelation:  $\theta_1 + \theta_{-1} = 2\theta_0$ .

Now we can self-consistently solve for the phases of all comb lines from Eq. (14), referenced to the pump phase  $\theta_0$ , giving

$$\theta_n = \theta_0 + n\phi. \quad (15)$$

This simple relation, while meant only to indicate the ideal limit of perfect phase locking (when phase mismatches are zero), is a useful guide in understanding the global behavior of the system.

## V. SEMICLASSICAL RAMAN MODULATOR MODEL

Because Eq. (5) describing all the Raman sidebands is difficult to solve, and the calculation in Sec. VI is only qualitative, we develop another supporting simplified approach, which we call the semiclassical Raman modulator model. This nonperturbative model assumes that the vibrational coherence (polarization) in the molecules is spontaneously created by the first Stokes and anti-Stokes mode pair, and the higher-order sidebands are generated by the action of this coherence back on the pump. Unlike the analysis in the previous section, here we use detailed mathematic derivations which allow us to gain further insight into the phase relations of all Raman sidebands.

The Raman pump field can be written as the sum of two classical-field components:

$$E = E^{(+)}e^{-i\omega_0 t} + E^{(-)}e^{i\omega_0 t}, \quad (16)$$

where (dropping various constants) the equation of motion for the positive-frequency part is [25]

$$(\partial_z + v_g \partial_t)E^{(+)} = iP^{(+)} = i\alpha(X)E^{(+)}. \quad (17)$$

In the previous equation we write the semiclassical electronic polarizability  $\alpha(X)$  as a function of internuclear coordinate  $X$ . Next, Taylor expand  $\alpha(X)$  around the equilibrium coordinate origin  $X_0$  and neglect the orders higher than the first term:

$$\alpha(X) \cong \alpha(X_0) + \left(\frac{\partial\alpha}{\partial X}\right)(X - X_0). \quad (18)$$

We discard the term  $\alpha_0(X)$ , as it affects only the phase velocity of the electric field. We also ignore for now any phase-velocity mismatching in this model. By changing to the local time variable  $z' = t - z/v_g$ , Eq. (17) can be written as

$$\partial_z E^{(+)} = i\alpha' X E^{(+)}, \quad (19)$$

where  $\alpha' = \left(\frac{\partial\alpha}{\partial X}\right)$ .

The electric field at the end of the Raman medium ( $z = L$ ) can be obtained by integrating the previous equation:

$$E^{(+)}(L, t) = E^{(+)}(0, t) \exp\left(i\alpha' \int_0^L dz' X(z', t)\right). \quad (20)$$

The  $X$  variable is related to the molecular polarization  $P$  created in the medium by [25]

$$\begin{aligned} X(z, t) &= P(z, t)e^{-i\omega_R t} + \text{H.c.} \\ &= 2|p(z, t)| \cos(\omega_R t + \varphi(z, t)), \end{aligned} \quad (21)$$

where  $\omega_R$  is the molecular resonance frequency, and  $\varphi(z, t)$  is the random phase variable arising from the Raman process. By putting Eq. (21) into Eq. (20), we get

$$\begin{aligned} E^{(+)}(L, t) &= E^{(+)}(0, t) \exp\left(i\alpha' \int_0^L dz 2|p(z, t)| \cos(\omega_R t + \varphi(z, t))\right) \\ &= E^{(+)}(0, t) \exp[i|a(t)| \cos(\omega_R t + \phi'(t))], \end{aligned} \quad (22)$$

where  $|a(t)|e^{i\phi'(t)} \equiv 2\alpha' \int_0^L dz |p(z, t)|e^{i\varphi(z, t)}$ . We use a mathematical expansion for the phase part of the previous equation, that is,

$$\exp(ix \cos(\beta)) = \sum_{n=-\infty}^{\infty} i^n J_n(x) \exp(in\beta),$$

and we use  $J_{-n}(x) = (-1)^n J_n(x)$  to rewrite  $J_n(x) = (-1)^n J_{|n|}(x)$ . Then

$$\begin{aligned} E^{(+)}(L, t) &= E^{(+)}(0, t) \sum_{n=-\infty}^{\infty} (-i)^n J_{|n|}(|a(t)|) \exp(in(\omega_R t + \phi'(t))) \\ &= E^{(+)}(0, t) \sum_{n=-\infty}^{\infty} J_{|n|}(|a(t)|) \exp(in(\omega_R t + \phi'(t) - \pi/2)). \end{aligned} \quad (23)$$

If we write  $\phi(t) = \phi'(t) - \pi/2$ , then

$$\begin{aligned} E^{(+)}(L, t) &= E^{(+)}(0, t) \sum_{n=-\infty}^{\infty} J_{|n|}(|a(t)|) \exp(in\phi(t)) \\ &\quad \times \exp(in\omega_R t). \end{aligned} \quad (24)$$

We can identify the complex amplitudes of the Stokes and anti-Stokes lines as

$$E_n^{(+)}(L, t) = E^{(+)}(0, t) J_{|n|}(|a(t)|) \exp(in\phi(t)).$$

We see that the first-order Stokes ( $n = 1$ ) and anti-Stokes ( $n = -1$ ) fields are predicted to have opposite phases, which is the same conclusion we derived earlier from the more rigorous quantum theory for the case of only two sidebands. Equation (24) is similar to the one derived in Ref. [2], except that here only a single pump is used and the effects of quantum fluctuations (ignored in [2]) are paramount. More interestingly, Eq. (24) predicts that the higher orders of Stokes and anti-Stokes fields will have their temporal phases related to the phase of the strong pump ( $\theta_0$ ) by

$$\theta_n = \theta_0 + n\phi(t). \quad (25)$$

Under high-gain transient conditions, the phase  $\phi(t)$  will be essentially constant during a single pulse, as discussed earlier. Therefore, this prediction is the same as obtained in Eq. (15) using a distinct and more qualitative argument. It can be understood, since higher-order sidebands arise from multiple scattering from the Raman medium. Each time the field gets scattered, the Raman medium will impose a  $\phi$  phase shift onto it.

## VI. PROSPECTS FOR ULTRASHORT PULSE GENERATION

Combining the ideal relation (25) with the frequency relations [shown in Eq. (1)], we find that the generated comb spontaneously satisfies the required relations for Fourier synthesis to create a periodic wave form. In order to see that, express the synthesized wave form as

$$\begin{aligned} E^{(+)}(t) &= \sum_n |E_n^{(+)}(t)| e^{i[(\omega_p + n\omega_R)t + n\phi + \theta_0]} \\ &= e^{i\omega_p t + i\theta_0} \sum_n |E_n^{(+)}(t)| e^{in(\omega_R t + \phi)}, \end{aligned} \quad (26)$$

where we assumed  $\phi(t) = \phi$  is constant during a given pulse (although random shot to shot). The intensity will be determined by the summation term, which is invariant with period  $T = 2\pi/\omega_R$  under the assumption that  $E_n$  is a slowly changing envelope compared to that period.

However, the carrier envelope phase of the synthesized wave form is changing, as we can see from Eq. (26), in which the term  $e^{i\omega_p t}$  is generally not invariant over period  $T$ . If the pump is tuned and stabilized to a multiple of the molecular resonance frequency [i.e.,  $\omega_p = m\omega_R$  ( $m$  is an integer)], then one set (train) of periodic pulses with constant CEP will be created within one pump pulse. On the other hand, because the quantum phase  $\phi$  changes from shot to shot, the pulse trains within successive laser shots will not have the same wave form and will not comprise isolated short pulses. Further locking mechanisms, such as coherent injection of molecular coherence, have been used to overcome this limitation, and stable ultrashort pulse trains were created, with the cost of added experimental complexity [6].

We are presently exploring whether simultaneous pumping of the medium by a fundamental pump and its phase-locked second harmonic, as in [6], but without external injection of coherence, can also lead to stable ultrashort pulse trains by a generalization of the phase locking discussed in the present paper. If the frequency of the fundamental pump is tuned to be precisely an integer multiple of the molecular resonance frequency, the doubled pump will be resonant with one of the anti-Stokes fields. For example, if we choose hydrogen molecules as our Raman medium, the vibrational resonance frequency is around 125 THz [9]. We can tune the pump to about 375 THz (or 802 nm), which is in the range of commonly used Ti-sapphire lasers. The frequency-doubled pump (401 nm) will be resonant with the third anti-Stokes field and will have a deterministic temporal phase  $\Delta\phi$  relative to the pump. Both the pump and its frequency-doubled beam will simultaneously interact with hydrogen molecules to generate the comb. The question is whether this will deterministically lock the temporal phase difference among adjacent comb lines, which is  $\phi$  in Eq. (25), to the value  $\Delta\phi/3$ , the only value that allows a self-consistent phase anticorrelation between all comb lines. The produced periodic single-cycle pulse trains will then be identical upon subsequent pump pulses.

## VII. CONCLUSIONS AND DISCUSSIONS

By developing a quantum theory of spontaneous Raman comb generation, we predict that the first-order Stokes and

anti-Stokes fields are automatically and strongly phase anti-correlated. We explained the mechanism of this phase locking by qualitatively exploring the conditions that maximize the molecular polarizations (coherence) in the generation process. This intuitive model is further extended using a semiclassical phase-modulation model, which is rooted in the quantum theory, to analyze the higher-order sidebands. Our analysis shows that the single-pump scheme is perhaps capable of producing periodic trains of subfemtosecond pulses. This result confirms the conjecture we previously outlined in [9].

It appears that both the benefit and the drawback of this scheme lie in the quantum spontaneous initiation of the Raman process. While the spontaneous nature of the generation tends to favor the desired phase (anti)correlations, the overall temporal phase of a generated Raman comb [ $\phi$  in Eq. (26)] would fluctuate from one pump pulse to another, and would result in different CEP of synthesized pulse trains. In order to overcome this uncertainty, we proposed to use an auxiliary beam, which is the frequency-doubled pump, to simultaneously pump the Raman comb generation.

In our simplified analysis for higher-order comb components in Sec. VI, there are some limitations that need to be addressed in future research. First, the dispersion in the medium for different comb components was ignored. Second, the time dependence of the random phase variable  $\phi$  was not fully considered. Third, a self-consistent solution for  $X$  in Eq. (21) was not used. It is likely that numerical simulations will be required to fully model these aspects.

## ACKNOWLEDGMENTS

This work has been supported by US National Science Foundation Grant No. PHY-0757818, and United Kingdom Engineering and Physical Sciences Research Council Grant No. EP/E039162/1.

## APPENDIX A

Here we derive the equations of motion for the slowly varying electric-field operators and the collective molecular raising operator. As stated in the main text, the effective interaction Hamiltonian is

$$\begin{aligned} H_I &= - \sum_n \int (NA) dz \{ \alpha_{1,n} P(z,t) E_n^{(+)}(z,t) E_{n-1}^{(-)}(z,t) e^{i\Delta\beta_n z} \\ &\quad + \alpha_{1,n+1}^* P^\dagger(z,t) E_n^{(+)}(z,t) E_{n+1}^{(-)}(z,t) e^{-i\Delta\beta_{n+1} z} \}. \end{aligned} \quad (A1)$$

Here the negative-frequency part of the slowly varying field operator is related to the spatially localized photon creation operator by

$$E_n^{(-)}(z,t) = i\sqrt{\frac{2\pi\hbar\omega_n}{AL}} a_n(z,t), \quad (A2)$$

and the molecular raising operator again is defined as

$$P(z,t) = 1/(NA) \sum_{\{m\}_z} \sigma_{31}^m(t), \quad (A3)$$

where summation is over all molecules located at position  $z$ . The commutation relations between different operators

are

$$[E_n^{(+)}(z,t), E_m^{(-)}(z',t')] = \delta_{nm} \frac{2\pi\hbar\omega_n}{A} \delta(z - z' - c(t - t')), \quad (\text{A4.a})$$

$$[P^\dagger(z,t), P(z',t)] = \frac{1}{NA} \delta(z - z'). \quad (\text{A4.b})$$

All other commutators are zero. The Heisenberg equation of motion for the negative-frequency part of the field operator is obtained by calculating its commutation with the total Hamiltonian:

$$\partial_t E_n^{(-)}(z,t) = i[H_0 + H_I, E_n^{(-)}(z,t)], \quad (\text{A5})$$

where  $H_0$  is the Hamiltonian of the electric fields in free space. It can be shown that this free-space Hamiltonian can be written as [neglecting other terms that commute with operator  $E_n^{(-)}(z,t)$ ] [26]:

$$H_0 = \frac{ic}{4\pi\omega_0} \int Adz \frac{\partial E_n^{(-)}(z,t)}{\partial z} E_n^{(+)}(z,t) + \text{H.c.} \quad (\text{A6})$$

Using this and the commutator (A4.a) in the equation of motion, we find

$$\partial_t E_n^{(-)}(z,t) = -c \partial_z E_n^{(-)}(z,t) + i[H_I, E_n^{(-)}(z,t)]. \quad (\text{A7})$$

The second term in (A7) is obtained by using the commutation relations:

$$\begin{aligned} & i[H_I, E_n^{(-)}(z,t)] \\ &= -i \left[ \sum_{n'} \int (NA) dz' \{ \alpha_{1,n'} P(z',t) E_n^{(+)}(z',t) E_{n'-1}^{(-)}(z',t) \right. \\ & \quad \times e^{i\Delta\beta_n z'} + \alpha_{1,n'+1}^* P^\dagger(z',t) E_n^{(+)}(z',t) E_{n'+1}^{(-)}(z',t) \\ & \quad \left. \times e^{-i\Delta\beta_{n+1} z'} \}, E_n^{(-)}(z,t) \right] \\ &= -i \left\{ NA \alpha_{1,n} P(z,t) \left( \frac{2\pi\hbar\omega_n}{A} \right) E_{n-1}^{(-)}(z,t) e^{i\Delta\beta_n z} \right. \\ & \quad \left. + NA \alpha_{1,n+1}^* P^\dagger(z',t) \left( \frac{2\pi\hbar\omega_n}{A} \right) E_{n+1}^{(-)}(z,t) e^{-i\Delta\beta_{n+1} z} \right\} \\ &= -i c \alpha_{2,n}^* P E_{n-1}^{(-)} \exp(i\Delta\beta_n z) - i c \alpha_{2,n+1} P^\dagger E_{n+1}^{(-)} \\ & \quad \times \exp(-i\Delta\beta_{n+1} z), \end{aligned}$$

where  $\alpha_{2,n} = 2\pi\hbar N \omega_n \alpha_{1,n}^* / c$ .

Then the equation of motion for the slowly varying electric-field operator is

$$\left( \partial_z + \frac{1}{c} \partial_t \right) E_n^{(-)}(z,t) = -i \alpha_{2,n+1} E_{n+1}^{(-)} \exp(-i\Delta\beta_{n+1} z) P^\dagger - i \alpha_{2,n}^* E_{n-1}^{(-)} \exp(i\Delta\beta_n z) P. \quad (\text{A8})$$

In same way, the equation of motion for the molecular raising operator can be found:

$$\begin{aligned} \partial_t P^\dagger(z,t) &= i[H_I, P^\dagger(z,t)] \\ &= -i \left[ \sum_n \int (NA) dz' \{ \alpha_{1,n} P(z',t) E_n^{(+)}(z',t) \right. \\ & \quad \left. \times E_{n-1}^{(-)}(z',t) e^{i\Delta\beta_n z'} + \alpha_{1,n+1}^* P^\dagger(z',t) E_n^{(+)}(z',t) \right. \end{aligned}$$

$$\begin{aligned} & \left. \times E_{n+1}^{(-)}(z',t) e^{-i\Delta\beta_{n+1} z'} \}, P^\dagger(z,t) \right] \\ &= i \sum_n \alpha_{1,n} E_n^{(+)} E_{n-1}^{(-)} \exp(i\Delta\beta_n z). \end{aligned}$$

Changing variables to  $(z, \tau)$ , where  $\tau = t - z/c$ , this gives

$$\begin{aligned} \partial_z E_n^{(-)}(z, \tau)|_\tau &= -i \alpha_{2,n+1} E_{n+1}^{(-)} \exp(-i\Delta\beta_{n+1} z) P^\dagger \\ & \quad - i \alpha_{2,n}^* E_{n-1}^{(-)} \exp(i\Delta\beta_n z) P, \quad (\text{A9.a}) \end{aligned}$$

$$\partial_\tau P^\dagger(z, \tau)|_z = i \sum_n \alpha_{1,n} E_n^{(+)} E_{n-1}^{(-)} \exp(i\Delta\beta_n z), \quad (\text{A9.b})$$

which is Eq. (5) in the main text.

## APPENDIX B

Here we give the detailed expressions for the correlation coefficient  $C$  that is defined in Eq. (10), and for the intensity of the first-order Stokes and anti-Stokes fields, by using the solution of Eq. (7) and the initial conditions of Eq. (9). The Stokes intensity is

$$\begin{aligned} I_s(L, \tau) &= \langle E_{-1}^{(-)}(L, \tau) E_{-1}^{(+)}(L, \tau) \rangle \\ &= \frac{|\alpha_{2,a}|^2}{AN} |E_0(\tau)|^2 \int_0^L dz' |G_{13}(z'; \tau, 0)|^2 \\ & \quad + \frac{2\pi\hbar\omega_{+1} |\alpha_{2,s} \alpha_{1,a}|^2}{Ac} |E_0(\tau)|^2 \int_0^\tau d\tau' |E_0(\tau')|^2 \\ & \quad \times |G_{12}(L; \tau, \tau')|^2. \quad (\text{B1}) \end{aligned}$$

The anti-Stokes intensity is

$$\begin{aligned} I_a(L, \tau) &= \langle E_{+1}^{(-)}(L, \tau) E_{+1}^{(+)}(L, \tau) \rangle \\ &= \frac{2\pi\hbar\omega_{-1} |\alpha_{1,s} \alpha_{2,a}|^2}{Ac} |E_0(\tau)|^2 \int_0^\tau d\tau' |E_0(\tau')|^2 \\ & \quad \times |G_{21}(L; \tau, \tau')|^2. \quad (\text{B2}) \end{aligned}$$

The product of Eqs. (B1) and (B2) gives the denominator of correlation coefficient  $C$ , and its numerator is

$$\begin{aligned} & |\langle E_{-1}^{(-)}(L, \tau) E_{+1}^{(-)}(L, \tau) \rangle|^2 \\ &= \left| \frac{2\pi\hbar\omega_{+1} |\alpha_{1,s}|^2 \alpha_{2,s} \alpha_{2,a}^*}{Ac} |E_0(\tau)|^2 \int_0^\tau d\tau' |E_0(\tau')|^2 \right. \\ & \quad \left. \times G_{11}(L; \tau, \tau') G_{12}^*(L; \tau, \tau') \right|^2. \quad (\text{B3}) \end{aligned}$$

Since the operators  $E_{-1}^{(-)}(L, \tau)$  and  $E_{+1}^{(-)}(L, \tau)$  commute, the numerator can also be expressed by changing their order:

$$\begin{aligned} & |\langle E_{+1}^{(-)}(L, \tau) E_{-1}^{(-)}(L, \tau) \rangle|^2 \\ &= \left| -\frac{\alpha_{2,s} \alpha_{2,a}^*}{AN} |E_0(\tau)|^2 \int_0^L dz' G_{13}(z'; \tau, 0) G_{23}^*(z'; \tau, 0) \right. \\ & \quad \left. - \frac{2\pi\hbar\omega_{-1} |\alpha_{1,a}|^2 \alpha_{2,s} \alpha_{2,a}^*}{Ac} |E_0(\tau)|^2 \int_0^\tau d\tau' |E_0(\tau')|^2 \right. \\ & \quad \left. \times G_{12}(L; \tau, \tau') G_{22}^*(L; \tau, \tau') \right|^2. \quad (\text{B4}) \end{aligned}$$

We can then ensure the precision of our calculations by comparing the values of Eqs. (B3) and (B4).



- [1] H. Kawano, Y. Hirakawa, and T. Imasaka, *IEEE J. Quantum Electron.* **34**, 260 (1998).
- [2] S. E. Harris and A. V. Sokolov, *Phys. Rev. Lett.* **81**, 2894 (1998).
- [3] M. Y. Shverdin, D. R. Walker, D. D. Yavuz, G. Y. Yin, and S. E. Harris, *Phys. Rev. Lett.* **94**, 033904 (2005).
- [4] T. Suzuki, M. Hirai, and M. Katsuragawa, *Phys. Rev. Lett.* **101**, 243602 (2008).
- [5] W. J. Chen *et al.*, *Phys. Rev. Lett.* **100**, 163906 (2008).
- [6] Z.-M. Hsieh, C.-J. Lai, H.-S. Chan, S.-Y. Wu, C.-K. Lee, W.-J. Chen, C.-L. Pan, F.-G. Yee, and A. H. Kung, *Phys. Rev. Lett.* **102**, 213902 (2009).
- [7] F. Couny, F. Benabid, and P. S. Light, *Opt. Lett.* **31**, 3574 (2006).
- [8] F. Benabid, G. Antonopoulos, J. C. Knight, and P. St. J., Russell, *Phys. Rev. Lett.* **95**, 213903 (2005).
- [9] F. Couny, F. Benabid, P. J. Roberts, P. S. Light, and M. G. Raymer, *Science* **318**, 1118 (2007); Supporting online material for Ref. [9].
- [10] I. A. Walmsley and M. G. Raymer, *Phys. Rev. Lett.* **50**, 962 (1983).
- [11] S. J. Kuo, D. T. Smithey, and M. G. Raymer, *Phys. Rev. A* **43**, 4083(R) (1991).
- [12] Y. Y. Wang, C. Wu, F. Couny, M. G. Raymer, and F. Benabid, *Phys. Rev. Lett.* **105**, 123603 (2010).
- [13] Y. Y. Wang, F. Couny, P. S. Light, and F. Benabid, in *Quantum Electronics and Laser Science Conference*, OSA Technical Digest (Optical Society of America, 2009), paper CTuB4; C. Wu, E. Mondloch, M. G. Raymer, Y. Y. Wang, F. Couny, and F. Benabid, in *Quantum Electronics and Laser Science Conference*, OSA Technical Digest (CD) (Optical Society of America, 2010), paper QTuA5.
- [14] H. Otsuka, T. Uchimura, and T. Imasaka, *Opt. Lett.* **29**, 400 (2004).
- [15] M. G. Raymer and I. A. Walmsley, in *Progress in Optics*, edited by E. Wolf, Vol. 28 (North-Holland, Amsterdam, 1990), pp. 181–270.
- [16] M. G. Raymer, I. A. Walmsley, J. Mostowski, and B. Sobolewska, *Phys. Rev. A* **32**, 332 (1985).
- [17] M. Belsley, D. T. Smithey, K. Wedding, and M. G. Raymer, *Phys. Rev. A* **48**, 1514 (1993).
- [18] J. R. Ackerhalt and P. W. Milonni, *Phys. Rev. A* **33**, 3185 (1986).
- [19] M. G. Raymer and J. Mostowski, *Phys. Rev. A* **24**, 1980 (1981).
- [20] S. Ya. Kilin, *Europhys. Lett.* **5**, 419 (1988).
- [21] M. D. Duncan, R. Mahon, J. Reintjes, and L. L. Tankersley, *Opt. Lett.* **11**, 803 (1986).
- [22] I. A. Walmsley *et al.*, *Opt. Commun.* **53**, 137 (1985).
- [23] M. G. Raymer, *J. Mod. Opt.* **51**, 1739 (2004).
- [24] Robert W. Boyd, *Nonlinear Optics* (Academic Press, San Diego, 2003), Chap. 10.
- [25] J. Mostowski and M. G. Raymer, in *Contemporary Nonlinear Optics*, edited by G. P. Agrawal and R. W. Boyd (Academic Press, San Diego, 1992), Chap. 5.
- [26] Hermann A. Haus, *Electromagnetic Noise and Quantum Optical Measurements* (Springer, New York, 2000), Chap. 12.